22nd Annual Fellowship Symposium Utah NASA Space Grant Consortium

Orem UT, 9 May 2016

Effects of Radiation Heating on Additively Printed Hybrid Fuel Grain Oxidizer-To-Fuel Ratio Shift

Stephen L. Merkley[1] and Stephen A. Whitmore[2]
Utah State University, Logan, Utah, 84322

Utah State University has researched and developed a hybrid rocket system that uses a non-toxic, simple, and 3D printed plastic as the fuel. This plastic is ABS (acrylonitrile butadiene styrene) which is a common material used in pipe systems, automotive components, and toys such as Lego bricks. As a fuel, ABS has structural properties that outweigh other polymer fuels; has matching or better performance than most commonly used propellants; is an environmentally-friendly fuel; and is easily manufactured and assembled. Furthermore, Utah State University has developed a novel ignition technology for hybrid rocket systems that involves pyrolyzing a marginal portion of the ABS fuel into a vapor rich in hydrocarbons which, when introduced to an oxidizer, initiates rapid combustion. Thus, the system simply requires a valve and spark command which grants restart and throttle capability. Although this technology has the potential to become a game-changing propulsion system for both the launch vehicles and small satellite communities, its performance and stability are still relatively uncharacterized. Many tests have been implemented at Utah State University and the performance model continues to be improved still. Recently, we have conducted tests on smaller-scale motors suited towards small spacecraft and have noticed a surprising trend in the oxidizer-to-fuel (O/F) ratio. Most results for hybrid rocket performance indicate that this ratio increases as the fuel is burned away, meaning that the combustion product becomes more oxidizer-rich as the motor is being fired. However, the results from the smaller-scale motors indicate that the oxidizer-to-fuel ratio decreases as the fuel is burned away. We believe that this trend towards a more fuel-rich burn is due to a neglected radiation effect that enhances the fuel regression rate. The goal of this research is to investigate this phenomena through running extensive tests as well as redevelop the equations describing fuel regression rate.

Nomenclature

$\dot{m}_{ox}$	Oxidizer Mass Flow Rate
$\dot{m}_f$	Fuel Mass Flow Rate
G_{ox}	Oxidizer Mass Flux
ρ_f	Fuel Density
$\dot{r}$	Mean Longitudinal Regression Rate
a	Regression Rate Model Scale Factor
n	Regression Rate Model Burn Exponent
m	Regression Rate Model Burn Exponent
A_b	Burn Surface Area
A_c	Port Cross-sectional Area
D	Port Diameter
L	Port Length
$\dot{q}_f$	Heat Flux Density Due to Ablated Fuel
$\dot{q}_c$	Heat Flux Density Due to Convection

---

[1]Graduate Student, Mechanical and Aerospace Engineering, 720 Stewart Hill Court, Student

[2]Professor, Mechanical and Aerospace Engineering, 4130 Old Main Hill

American Institute of Aeronautics and Astronautics

$\dot{q}_r$	Heat Flux Density Due to Radiation
h_v	Fuel Enthalpy of Vaporization (Latent Heat)
Δh	Flame Surface Enthalpy Change
S_t	Non-Dimensional Stanton Number
ρ_e	Density of Combustion Product
U_e	Velocity of Combustion Product
c_p	Specific Heat at Constant Pressure of Combustion Product
T_0	Combustion Flame Temperature
T_f	Fuel Temperature
σ_B	Stefan Boltzmann Constant
ϵ	Optical Emissivity
α	Optical Absorbtivity
P_r	Non-Dimensional Turbulent Prandtl Number
C_f	Local Skin Friction Coefficient
C_{f_0}	Standard Skin Friction Coefficient Without Radial Wall Blowing
β	Lee's Blowing Coefficient
ρ_{wall}	Density of Boundary Layer Product
U_{wall}	Velocity of Boundary Layer Product
ρ_{ox}	Density of Oxidizer
U_{ox}	Velocity of Oxidizer
τ	Skin Friction Coefficient Scale Factor
R_e	Reynolds Number
μ	Dynamic Viscosity of Boundary Layer Product
x	Longitudinal Length Downstream of Injector
j	Iteration

Introduction

The discovery of the unique electrical breakdown characteristics inherent to ABS has prompted the invention of an ignition system that takes advantage of the pyrolysis-induced hydrocarbon seeding phenomena: demonstrating on-demand ignition using both nitrous oxide [1] and gaseous oxygen [2] as oxidizers. This arc-ignition method has been developed up to a technology readiness level (TRL) capable for flight-ready systems with multiple motor design configurations varying in size and thrust levels. Previous tests conducted at Utah State University [3] [4] have demonstrated that using medium scale ABS-fuel thrusters (800-250 N) produce nearly equivalent performance to the legacy fuel material, hydroxyl-terminated polybutadiene (HTPB), with only slightly lower mean regression rates and nearly identical specific impulse. However, although the mean regression rates are similar between these two thermoplastic fuels, ABS-fueled hybrid motors exhibit a significant drop in oxidizer-to-fuel (O/F) ratio and become increasingly more fuel-rich as the fuel port widens. This phenomenon is in contrast to HTPB fuel where it is well known that the O/F ratio increases during the burn.

The O/F ratio is expressed as the ratio of oxidizer mass flow to fuel mass flow. For a cylindrical fuel port,

$$O/F = \frac{\dot{m}_{ox}}{\dot{m}_f} = \frac{G_{ox}A_c}{\rho_f \dot{r}A_b} = \frac{G_{ox}D}{4\rho_f \dot{r}L} \tag{1}$$

Allowing a simple, Marxman-style regression rate model of the form,

$$\dot{r} = aG_{ox}^n L^m \tag{2}$$

Where a is a scale factor and n and m ($m \approx 1 - n$) are burn exponents, the O/F ratio can be further reduced to,

$$O/F = \frac{G_{ox}^{1-n}D}{4a\rho_f L^{m+1}} = \frac{\dot{m}_{ox}^{1-n}D^{2n-1}}{4^n\pi^{1-n}a\rho_f L^{m+1}} \tag{3}$$

Analysis of Eq. (2) shows that for a burn exponent of $n > 1/2$, the O/F ratio is progressive and increases as the fuel grain is burned away. Conversely, when $n < 1/2$, the O/F ratio is regressive and becomes increasingly fuel-rich with time. When $n \approx 1/2$, the burn rate is neutral and implies no O/F ratio shift during the burn. As shown by Figure (1),

other studies [5] of commonly used thermoplastic fuels all have burn exponents of $n > 1/2$, leading to fuel-lean burns. Thus, the behavior exhibited by printed ABS is a clear anomaly.
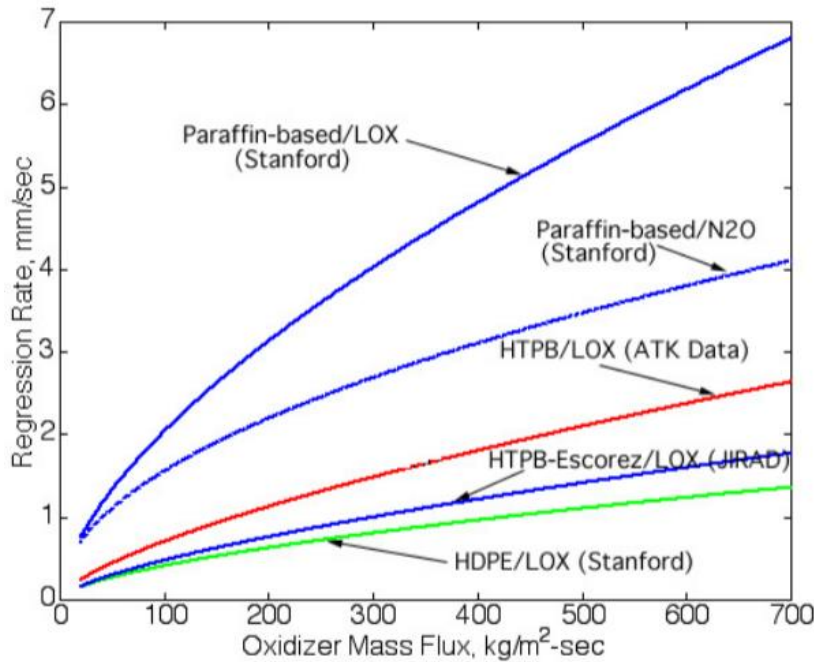
- **HTPB/LOX:**
$$\dot{r} = 3.043\ 10^{-2} G_{ox}^{0.681}$$

- **HTPB/Escorez/LOX**
$$\dot{r} = 2.061\ 10^{-2} G_{ox}^{0.68}$$

- **HDPE/LOX**
$$\dot{r} = 2.340\ 10^{-2} G_{ox}^{0.62}$$

- **Paraffin/LOX**
$$\dot{r} = 11.70\ 10^{-2} G_{ox}^{0.62}$$

- **Paraffin/N2O**
$$\dot{r} = 15.50\ 10^{-2} G_{ox}^{0.50}$$

(Units are mm/sec and kg/m²-sec)

Figure 1. Regression Rate Data for Various Hybrid Propellants

The quantitative behavior of ABS fuel also matches the qualitative physical observations, where the tendency towards a progressively fuel-rich burn are seen as the plume changes from a clean to sooty flame only 40-50% of the way through the fuel grain lifetime. The sequence of images shown in Figure (2) displays a series 2-second pulsed burns. For this test, the motor length was tuned to give an O/F ratio slightly greater than the stoichiometric point (~ 2.0) for the initial part of the burn, with the O/F ratio dropping to less than 0.5 by the end of the burn.

The postulation that initiates this research is based on accounting for additional radiative effects during the burn, which may explain the fuel-rich behavior of ABS. The original Marxman [6] model of Eq. (2) assumes that the fuel regression rate is a result of the convective heat transfer from the flame zone to the fuel wall. Because the radiative heat transfer from the flame zone to the fuel wall is considered to be negligible, motor size effects are also considered to be negligible, and the burn exponents are typically treated as constants that are matched to a given propellant combination. This is clearly an incomplete model when regarding small-scale motors with printed ABS propellant.
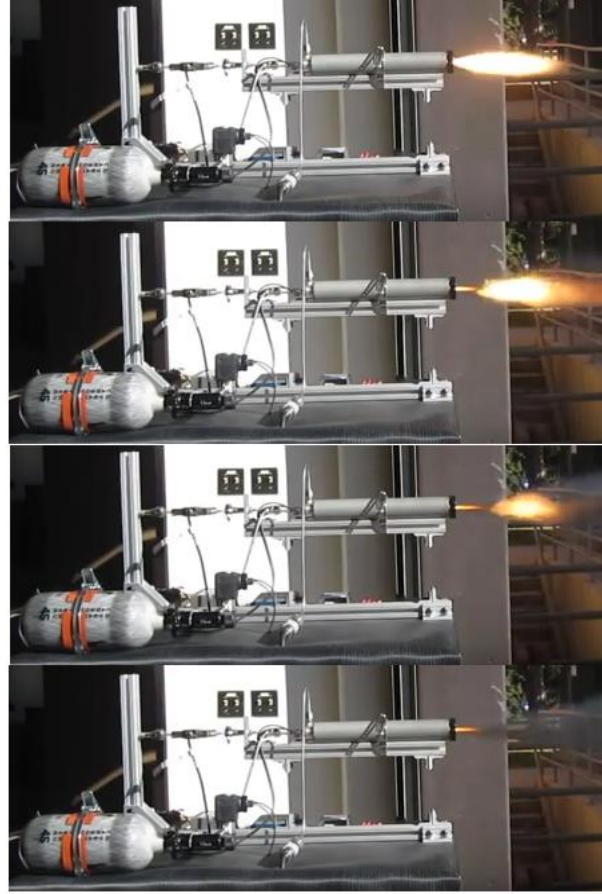
Figure 2. Image Sequence Demonstrating Progressive Fuel-Rich Behavior

Objectives

- **Proposed Radiation-Adjusted Model**

The radiation-adjusted model begins with the classical Marxman approach that balances the heat flux density of ablated fuel to the heat flux density due to convection. The difference now is that a new term accounting for heat flux density due to radiation is added. This enthalpy balance between convection, radiation, and fuel ablation is,

$$\dot{q}_f = \dot{q}_c + \dot{q}_r \tag{4}$$

Where the heat flux density of ablation, convection, and radiation, respectively, is,

$$\dot{q}_f = \rho_f \dot{r} h_v \tag{5}$$

$$\dot{q}_c = S_t \rho_e U_e c_p (T_0 - T_f) \tag{6}$$

$$\dot{q}_r = \sigma_B \left(\epsilon T_0^4 - \alpha T_f^4 \right) \tag{7}$$

The derivation initially ignores the effects of radiative heat transfer,

$$\dot{q}_f = \dot{q}_c \Rightarrow \rho_f \dot{r} h_v = S_t G_{ox} \Delta h \tag{8}$$

Where the product of the combustion material density and velocity is assumed to be equivalent to the oxidizer mass flux ($\rho_e U_e = G_{ox}$), and the flame surface enthalpy change is equivalent to the product of the specific heat constant and the difference between the combustion temperature and fuel temperature ($\Delta h = c_p(T_0 - T_f)$). The Stanton number is written in terms of the local skin friction coefficient using the Reynold-Coburn Analogy [7],

$$S_t = \frac{C_f}{2 P_r^{\frac{2}{3}}} \tag{9}$$

Substituting Eq. (9) into Eq. (8) and solving for the regression rate, we have the regression rate written in terms of the local skin friction coefficient,

$$\dot{r} = \left(\frac{G_{ox}}{2 P_r^{\frac{2}{3}} \rho_f} \right) \left(\frac{\Delta h}{h_v} \right) C_f \tag{10}$$

In order to account for a radially emanating flow field, Boardman's [8] model of the skin friction coefficient is implemented. This alternate form of the skin friction coefficient is as follows,

$$C_f = \frac{1.27 C_{f_0}}{\beta^{0.77}} \tag{11}$$

Where Lee's [8] blowing coefficient, β, is defined by,

$$\beta = \left(\frac{\rho_{wall} U_{wall}}{\rho_e U_e S_t} \right) \approx \frac{2 \dot{r} \rho_f}{G_{ox} C_{f_0}} \tag{12}$$

C_{f_0} is the standard skin friction coefficient without radial wall blowing and C_f is the skin friction coefficient as would occur with wall blowing. Substituting Eq. (12) into Eq. (11) and simplifying, the regression rate formula is written in terms of the standard skin friction coefficient as,

$$\dot{r} = \left(\frac{0.635}{\rho_f P_r^{\frac{2}{3}}} \right) \left(\frac{\Delta h}{h_v} \right) \left(\frac{(C_{f_0} G_{ox})^{1.77}}{(2 \dot{r} \rho_f)^{0.77}} \right) \tag{13}$$

Now the radiation term is added to correct the enthalpy balance model, producing a regression rate written as,

$$\dot{r} = \left(\frac{0.635}{\rho_f P_r^{\frac{2}{3}}} \right) \left(\frac{\Delta h}{h_v} \right) \left(\frac{(C_{f_0} G_{ox})^{1.77}}{(2 \dot{r} \rho_f)^{0.77}} \right) + \frac{\sigma_B (\epsilon T_0^4 - \alpha T_f^4)}{\rho_f h_v} \tag{14}$$

The skin friction coefficient is evaluated using a generic Reynolds number model of the form,

$$C_f = \frac{\tau}{R_e^{1-n}} = \tau \left(\frac{\rho_{ox} U_{ox} x}{\mu} \right)^{n-1} = \tau G_{ox}^{n-1} \left(\frac{\mu}{x} \right)^{1-n} \tag{15}$$

Substituting Eq. (15) into Eq. (14) and simplifying,

$$\dot{r} = \left(\frac{0.635\tau}{\rho_f P_r^{\frac{2}{3}}}\right)\left(\frac{\Delta h}{h_v}\right)\left(G_{ox}^n\left(\frac{\mu}{x}\right)^{1-n}\right)\left(\frac{\tau G_{ox}^n\left(\frac{\mu}{x}\right)^{1-n}}{2\rho_f\dot{r}}\right)^{0.77} + \frac{\sigma_B\left(\epsilon T_0^4 - \alpha T_f^4\right)}{\rho_f h_v} \tag{16}$$

The solution for the radiation-adjusted regression rate proceeds iteratively, where j is the iteration number,

$$\beta^{(j)} = \frac{2\rho_f\dot{r}^{(j)}}{\tau G_{ox}^n\left(\frac{\mu}{x}\right)^{1-n}}$$

$$\dot{r} = \left(\frac{0.635\tau}{\rho_f P_r^{\frac{2}{3}}}\right)\left(\frac{\Delta h}{h_v}\right)\left(G_{ox}^n\left(\frac{\mu}{x}\right)^{1-n}\right)\left(\frac{1}{\beta^{(j)}}\right)^{0.77} + \frac{\sigma_B\left(\epsilon T_0^4 - \alpha T_f^4\right)}{\rho_f h_v} \tag{17}$$

This model will be verified by how well it fits the trend shown from the experimental data.

- **Effect of Radiation Heating on Motor O/F Shift**

The O/F shift is modeled using Eq. (17) as,

$$O/F = \frac{G_{ox}\pi D^2}{2\rho_f\pi DL\dot{r}} \tag{18}$$

Plugging in the expression for $\dot{r}$ and reducing,

$$\left(\frac{O}{F}\right)^{-1} = D^{1-2n}\left(\frac{0.0376}{\rho_f P_r^{\frac{2}{3}}}\right)\left(\frac{\Delta h}{h_v}\right)\left(\frac{1}{\beta^{(j)}}\right)^{0.77}\left(\frac{4\dot{m}_{ox}}{\pi}\right)^{n-1}\left(\frac{\mu}{x}\right)^{1-n} + \frac{\pi D\sigma_B\left(\epsilon T_0^4 - \alpha T_f^4\right)}{4\dot{m}_{ox}\rho_f h_v} \tag{19}$$

Inspection of Eq. (19) leads to an interesting result: for $n > 1/2$, the convective term gets fuel lean with time as the port diameter grows and the radiation term gets fuel rich with time as the port diameter grows. For $n < 1/2$, both the convective and radiation terms get fuel rich as the port diameter grows. This is to say that for lower burn exponents – which is the empirical trend observed in small-scale ABS motors – the convection within the chamber decreases the O/F ratio. One could say that this is due to a smaller fuel port which causes ablated fuel to saturate the chamber instead of a larger fuel port that allows room for fuel to be exhausted along the flow path. Furthermore, at low mass flux levels, the radiation term dominates: tending towards a fuel rich burn. While at higher mass flux levels, the convective term dominates: tending towards a fuel lean burn.

- **Experimental Campaign**

Preliminary tests have already been completed in order to demonstrate the progressive fuel-rich trend in small-scale motors using ABS fuel. Figure (3) compares the oxidizer mass flux as a function of O/F ratio for 98, 75, 54, and 38mm diameter motors.
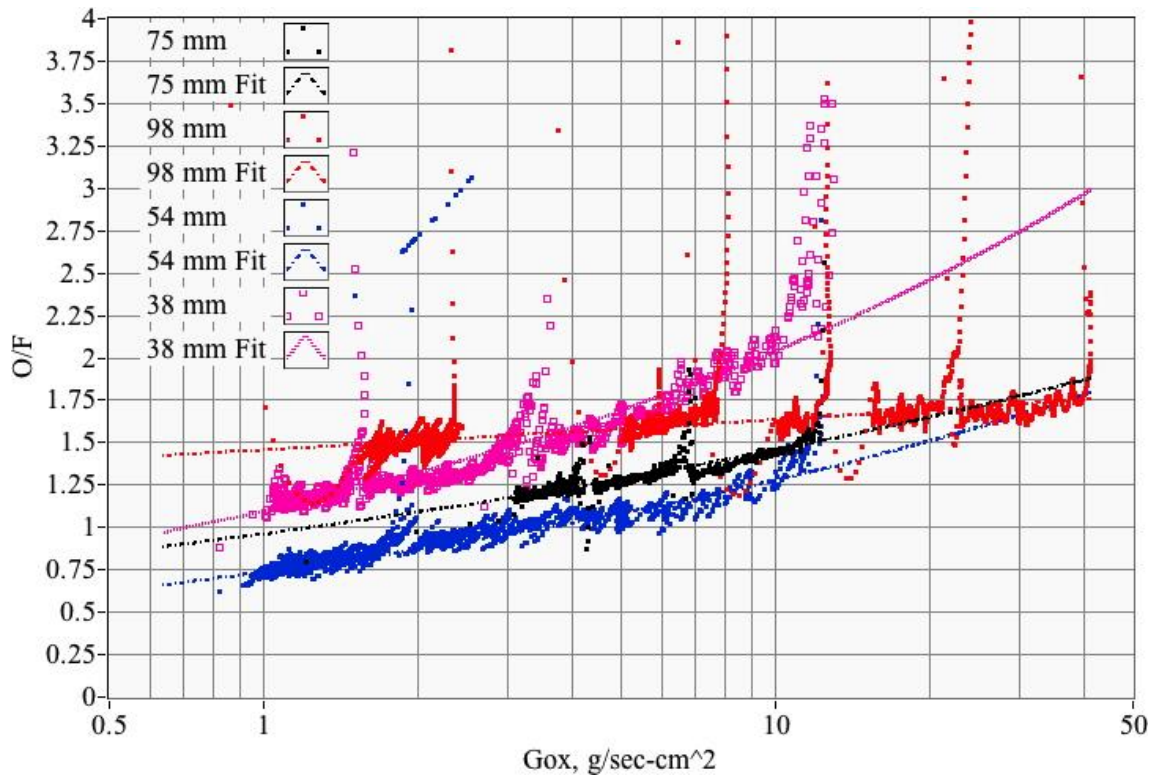
American Institute of Aeronautics and Astronautics

Figure 3. Oxidizer Mass Flux as a Function of O/F Ratio for Different Motor Diameters

Despite the scarce amount of tests carried out on the 38mm motor, the regressive O/F is already apparent as the oxidizer mass flux decreases (as the port widens). In addition to the results shown in Figure 3, tests were run at different oxidizer pressures for both the 38mm motor and a 29mm motor. At the time of this paper, the data is being processed with preliminary results confirming the O/F trend further.

Future Work before Final Publication

The model of Eq. (17) is being used to adjust the previously collected data for radiation effects in order to understand the relative contributions of the convective and radiative heat transfer terms with regard to the fuel regression rate. This analysis will test the hypothesis that the observed scale effects on the O/F shift are either primarily the result of the radiative heat transfer contribution, the choice of additively-manufactured ABS as the fuel material, or a combination of both effects. The iterative process will start with the currently derived burn exponents, and then iteratively adjust for the effects of radiative heat transfer using the algorithm of Eq. (19). A range of appropriate values for emissivity and absorptivity will be considered. Revised, radiation-adjusted burn exponents for the regression rate/oxidizer mass flux curve will be recalculated. Effects of total mass flux on the regression rates will also be examined.

Conclusion

Additively-printed ABS fuel and Utah State University's arc-ignition technology has potential game-changing characteristics in the hybrid rocket community as well as in the entirety of chemical propulsion, including low cost, low power, non-toxicity, system simplicity, and ease of manufacturing, producing, and handling. But these benefits will never be completely realized until ABS fuel performance can be modeled and predicted. There also exists myriad properties that have yet been studied, such as print density, fuel regression as a function of axial length, and chemical kinetics. This research, along with the research conducted in the past and the research that will continue, contribute to the Technology Readiness Level (TRL) enhancement effort of using additively-printed ABS in hybrid rockets and thrusters.

References

[1] Stephen A. Whitmore. "Additively Manufactured Acrylonitrile-Butadiene-Styrene–Nitrous-Oxide Hybrid Rocket Motor with Electrostatic Igniter", *AIAA J. Propulsion and Power* r, Vol. 31, No. 4 (2015), pp. 1217-1220.

[2] Stephen A. Whitmore, Nathan Inkley, and Daniel P. Merkley, "Development of a Power-Efficient, Restart-Capable Arc Ignitor for Hybrid Rockets", *AIAA J. Propulsion and Power*, Vol. 31, No. 6 (2015), pp. 1739-1749.

[3] Whitmore, Stephen A., Peterson, Zachary W., and Eilers, Shannon D., "Comparing Hydroxyl Terminated Polybutadiene and Acrylonitrile Butadiene Styrene as Hybrid Rocket Fuels," *AIAA J. Propulsion and Power*, vol. 29, no. 3, May–June 2013.

[4] Stephen A. Whitmore, Sean D. Walker, Daniel P. Merkley, and Mansour Sobbi. "High Regression Rate Hybrid Rocket Fuel Grains with Helical Port Structures", *AIAA J. Propulsion and Power*, Vol. 31, No. 6 (2015), pp. 1727-1738.

[5] Arif Karabeyoglu, "Lecture 10 Hybrid Rocket propulsion Design Issues," AA 284a Advanced Rocket Propulsion, AAE Department, Stanford University, May 14, 2012, p. 18, http://www.spg-corp.com/docs/Stanford_AA284a_Lecture10.pdf, [Retrieved 01 January, 2016].

[6] Marxman, G. and M.Gilbert, "Turbulent boundary layer combustion in the hybrid rocket," *Symposium (International) on Combustion*, Vol. 9, No. 1., 1963, pp. 371–383.

[7] White, Frank M., *Viscous Fluid Flow*, McGrawHill, Inc., New York, 1991, pp. 485-486.

[8] Lees, L., "Convective Heat Transfer with Mass Addition and Chemical Reactions," *Combustion and Propulsion, 3rd AGARD Colloquium*, New York, Pergamon Press, 1958, p. 451.